Internal Report
DESY M-95-01
January 1995

Investigations of Field Asymmetries in the Asymmetric Input Coupler of the e^+e^- Injector Linac at DESY

by

S.V. Ivanov

Moscow Engineering Physics Institute
Kashirskoe shosse 31, 115 409 Moscow, Russia

M. Dohlus, N. Holtkamp

Deutsches Elektronen Synchrotron DESY
Notkestraße 85, 22607 Hamburg, Germany

INVESTIGATIONS OF FIELD ASYMMETRIES IN THE ASYMMETRIC INPUT COUPLER OF THE e^+e^- INJECTOR LINAC AT DESY.

S. Ivanov, *Moscow Engineering Physics Institute, MEPI*
Kashirskoe shosse,31, 115409 Moscow, Russia

M. Dohlus, N. Holtkamp, *Deutsches Elektronen-Synchrotron, DESY*
Notkestraße 85, 22607 Hamburg, Germany

Abstract

A prototype input coupler for the S-band injector linac at DESY (LINAC II) has been designed based on MAFIA field calculations. The symmetric coupler with two waveguides, one connected to the RF source and the other to the vacuum system, could be matched without changes in geometry by adjusting an RF-reflector in the vacuum waveguide. The field asymmetries in the coupler cell were measured and have been compared to our numerical predictions. In conventional one-waveguide-couplers the amplitude asymmetry is compensated by shifting the coupler cell transversally while the phase asymmetry cannot be influenced. For the two-waveguide-coupler the same effect can be achieved without a shift by simultaneous tuning of the coupler cavity and the reflector position. This is demonstrated by measurements and calculations.

1. Introduction.

The injector linac at DESY (LINAC II) consists of twelve traveling wave sections, each powered by a 25 MW klystron with a pulse compression system (SLED). These sections were built in 1972 by Varian Associates, Palo Alto, California [1]. The sections are 5.2 meters long and have an integrated load [2] over a length of 26 cm which absorbs rf power at the end of the accelerating section while still accelerating the beam. Due to corrosion caused by the water cooling the sections will be replaced by a new design. The new sections are continuously tapered with a linear variation of the group velocity from $0.037c_0$ to $0.0136c_0$. They have an integrated load also, but no vacuum envelope. Therefore the input coupler has two purposes: to couple to the rf and to the vacuum system. In the first design step, the coupler is symmetrical with two coupling holes as shown in fig. 1. An input hole is intended for the input power and a hole N2 for the vacuum pump. An rf reflector in the vacuum waveguide protects the vacuum system from the rf power and provides a clearly defined rf termination. With the exception of the iris and the hole to the beam-pipe, the coupler is flat and has only convex edges parallel to the beam axis. This omits field maximums caused by edge effects and simplifies the numerical field analysis. The structure can be calculated either completely in three dimensions or by independent 2D runs for the rotationally symmetric and for the flat part. The 2D

calculations are related by an expansion in cylindrical functions and enable a good spatial resolution with low numerical effort.

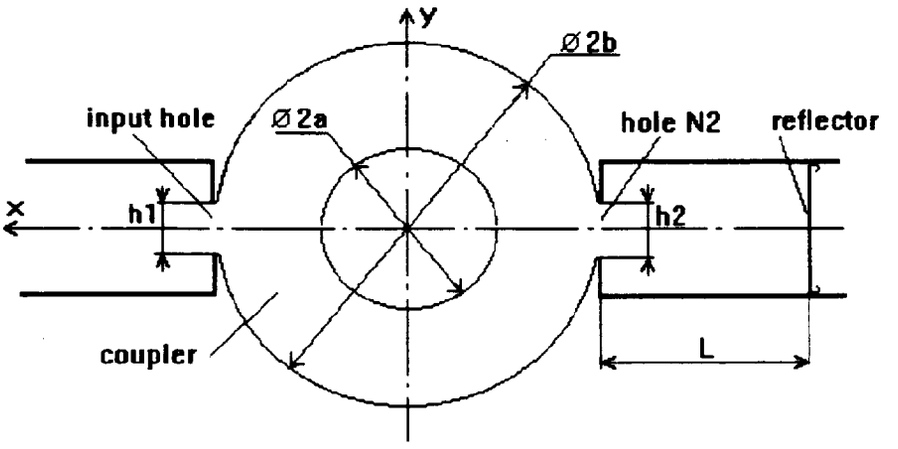

Fig. 1. The geometry of the input coupler of the DESY LINAC II ($2a$=29,77 ; 2b=77,6 ; h_1=h_2=31,04).

By this method the dimensions in fig. 1 have been determined and other possible triples of b, $h_1 = h_2$, L can be evaluated. The configuration has one degree of freedom that will be used later to optimize the field symmetry. As $h_1 = h_2$ is almost independent on the other two parameters, it is possible to investigate several modes of operation with an almost matched coupler when the cavity frequency and the reflector position can be tuned arbitrarily.

2. Measurement of the field asymmetry in the input coupler.

To measure the field asymmetry in the coupler we need a traveling wave in the structure and therefore a good load at the end of the structure. As a first step, we try to obtain the traveling wave in the constant impedance structure υ_g/c=3,7%.

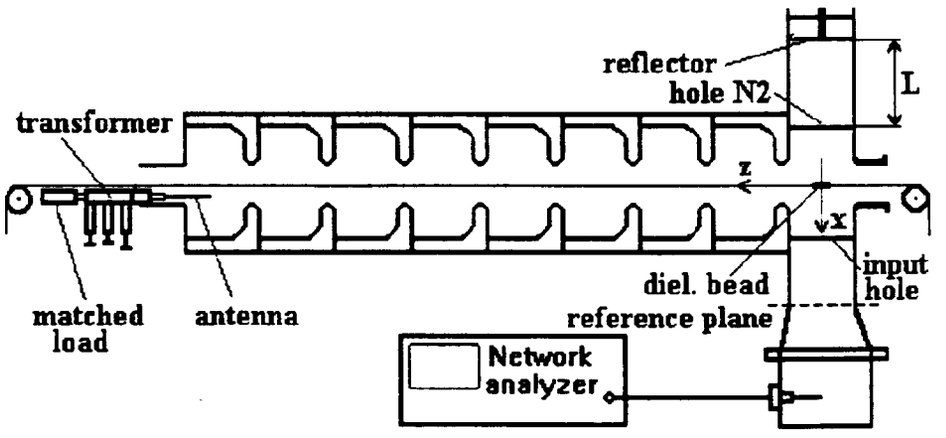

Fig. 2. The scheme of the field distribution measurement of the traveling wave in the constant impedance structure υ_g/c =3,7%.

This scheme is shown in Fig. 2. Standard elements (a coaxial transformer and a matched coaxial load) without absorbent elements in the structure are used. An antenna is set at the end of the structure and joined by a coaxial transformer with the coaxial load. By simply changing the reflection coefficient of the coaxial load by means of the transformer, we can obtain the required value at the coupler iconocenter in the reference plane. That means that in this reference plane the reflection is caused by the coupler only and not by the structure. Therefore, there is a traveling wave in the structure. We can observe this easily by measuring the field distribution by a non-resonant perturbation method [3]. By moving the dielectric body with dimensions: length l=5 mm, diameter d=1 mm and $\varepsilon<9$ along the structure we get the distribution of the field shown in Fig. 3.

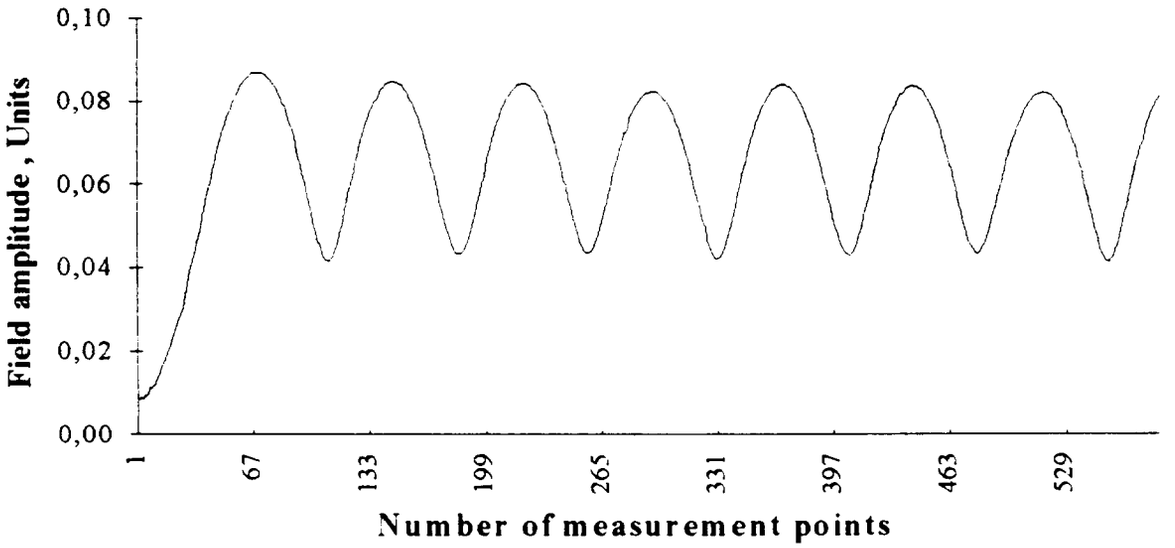

Fig. 3. The traveling wave field distribution in the structure.

The field amplitude is approximately 5% higher in the coupler cell than in the next cells and has a periodical variation as typical for a traveling wave. The higher field strength in the coupler is a consequence of the fixed cell length and phase advance. In the later cells one can observe a 3-cell-subperiod that indicates a standing wave ratio of 1.02...1.03 .

Then the field asymmetry is investigated by moving the dielectric body parallel to the longitudinal axis of the structure (z-axis) with a x-offset that is a multiple of ±3mm. The results obtained are shown in figures 4, 5. In the beam pipe, the coupler cell and close to the irises the amplitude has a significant dependency on the transverse position. Table 1 and the transversal plot in fig. 6 show that the field in the coupler cell is asymmetric while it is almost perfectly symmetric in the next cell. The field symmetry in the cells after the coupler is a criterion of the correct measurement. The phase distribution in fig.5 is nearly constant in the beam pipe, where we are in a standing wave regime, is flat in the middle of all cells and varies rapidly in the irises. Then the influence of position errors on the measurement of the cell to cell phase shift

is minimal in the middle planes. The asymmetry in the coupler is documented in table 2 and fig.7.

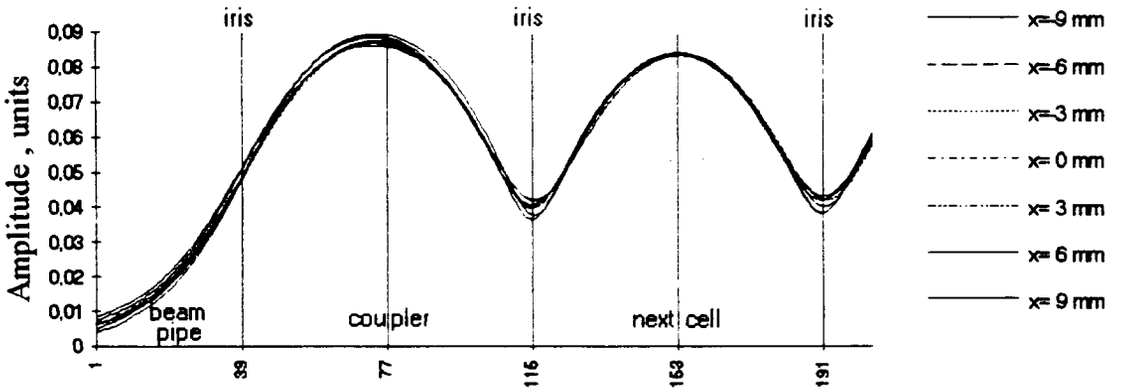

Fig. 4. Field distribution along the z-axis in the coupler and in the next cell with different x-offsets

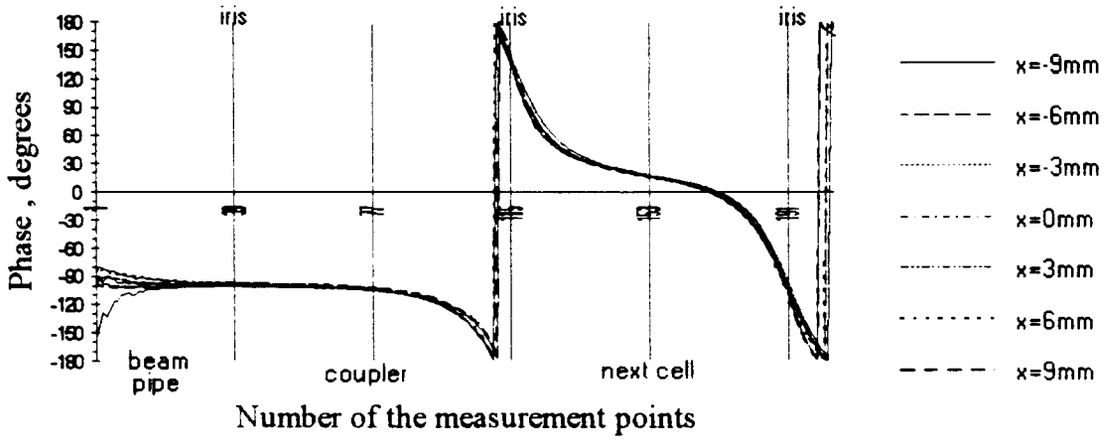

Fig. 5. The phase distribution along the z-axis in the coupler and in the next three cells with different x offsets.

Table 1 Amplitude along x-axis (Units)

x	coupler			next cell
	z=0	z=-4.33	z=4.33	z=33.33
mm		mm	mm	mm
-18	0,08442	0,08429	0,08293	0,08444
-12	0,08591	0,08508	0,08197	0,08483
-9	0,08603	0,08466	0,08192	0,08421
-6	0,08670	0,08493	0,08205	0,08404
-3	0,08677	0,08475	0,08223	0,08370
0	0,08748	0,08550	0,08277	0,08353
3	0,08827	0,08694	0,08290	0,08375
6	0,08868	0,08728	0,08358	0,08381
9	0,08933	0,08746	0,08513	0,08388
12	0,09093	0,08936	0,08723	0,08483
18	0,09040	0,09026	0,08805	0,08469

Table 2. Phase along x-axis (degr.)

x	coupler			next cell
	z=0	z=-4.33	z=4.33	z=33.33
mm		mm	mm	mm
-18	-102,97	-102,15	-103,99	18,13
-12	-104,06	-102,30	-107,27	16,76
-9	-104,72	-102,79	-108,61	17,76
-6	-104,49	-102,17	-109,23	17,24
-3	-104,63	-102,25	-109,55	18,07
0	-104,13	-101,70	-109,07	17,38
3	-103,53	-101,03	-108,56	16,24
6	-102,88	-100,60	-107,62	16,56
9	-102,25	-100,16	-106,15	16,86
18	-97,99	-97,05	-99,36	17,47

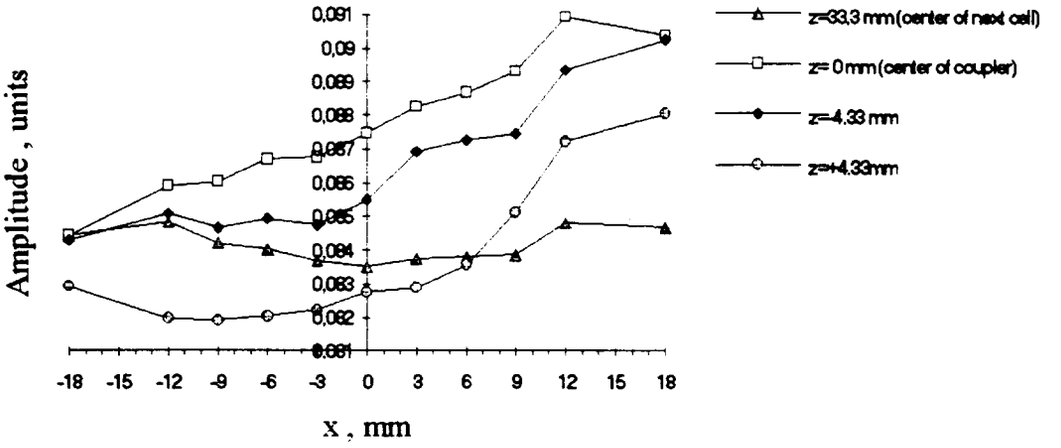

Fig. 6. Field amplitude along the x-axis in the coupler and the next cell.

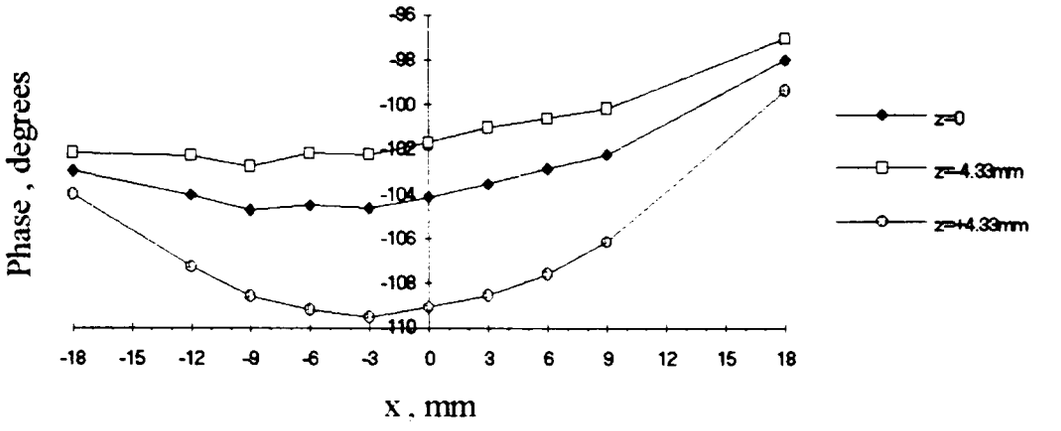

Fig. 7. Phase distribution along the x-axis in the coupler.

The asymmetry (A_a , %/mm) of the field amplitude is defined by:

$$A_a = 100\%*(\partial|E|/\partial x)/Eo = 100(|E_1|-|E_2|)/(E_o\Delta x) \ , \qquad (1)$$

with $E_o = |E(0)|$ - the amplitude in the point x=0 and $E_{1,2} = E(\pm\Delta x/2)$.

The phase asymmetry (A_{ph}, °) in the coupler is defined similarly:

$$A_{ph} = \partial \arg(E)/\partial x \approx (\arg(E_1) - \arg(E_2))/\Delta x \ , \qquad (2)$$

Additionally we introduce the total asymmetry (A_t) as:

$$A_t = 100\%*|\partial E/\partial x|/Eo = \sqrt{A_a^2 + (100\%*A_{ph}*\pi/180°)^2} \ , \qquad (3)$$

that describes the contribution of the asymmetry without respect to the phase of the accelerating field.

Table 3 summarizes the results of the asymmetry calculation by these formulas (1), (2) and (3) for the original geometry in fig. 1 . One can see, that the amplitude asymmetry in the coupler of approximately 0.2÷0.3% per mm is damped by one order to the next cell and agrees within the range of the measurement accuracy with the calculated value. The phase asymmetry is about 0.14÷0.18 ° per mm and is slightly underestimated by MAFIA. The total asymmetry (A_t. % mm) in the next cell after the coupler is less than 0.1 % per mm. This value is approximately the resolution of the measurement setup (0.1 %/mm ↔ 0.06 °/mm). The numerical calculation in fig.8a promises a drop to values less than 0.015 %/mm.

Table 3. Amplitude and phase asymmetries.

dx / mm	**Amplitude asymmetry, %/mm**				**Phase asymmetry, ° / mm**				**|Total asymmetry|, %/mm**			
	coupler			next	coupler			next	coupler			next
	z=0 mm	z=4.3 mm	z=-4.3 mm	cell	z=0 mm	z=4.3 mm	z=-4.3 mm	cell	z=0 mm	z=4.3 mm	z=-4.3 mm	cell
6	0.286	0.136	0.427	0.009	0.183	0.164	0.202	0.035	0.428	0.317	0.554	0.062
12	0.188	0.154	0.229	0.023	0.134	0.134	0.131	0.056	0.300	0.280	0.324	0.100
18	0.210	0.216	0.182	0.022	0.138	0.136	0.146	0.050	0.320	0.320	0.313	0.090
MAFIA-2D	0.29				0.12				0.35			0.015

From fig. 8 it is obvious, that the longitudinal antisymmetric field $Ea=[E_z(+x)+E_z(-x)]/2$ and the transverse field are in the same order in the central plane of the coupler. In every other plane the transverse field is much higher. This has of course no effect on the beam, because the transverse wake of monopole modes vanishes, but it is important for field measurements by the perturbation method. For example in the central plane of cell 2, the amplitude of the transversal field is approximately E_0*0.0085*x/0.8mm . If we assume that the perturbation probe is 5 times more sensitive to longitudinal than to transversal fields, than the effect of a transversal inaccuracy of 0.2 mm causes an asymmetry error of ~0.05 %/mm. This indicates the order of the measurement error of the values in table 3 and shows the relevance of these numbers.

3. Investigation of the influence of the coupler cell tuning and the reflector position on the field asymmetry.

All measurements in section 2 were done with the same size of the input hole and the N2 hole. During other investigations the width of the N2 aperture has been changed to $h_2=h_1+1.5$mm. Therefore the reflector had to be shifted by -1 mm to L=75 mm to achieve optimal tuning. In the new setup for traveling wave measurements (see fig.9) the coupler is connected to five standard cells (v_g/c = 3.7 %) and another type of matched load [4] that causes a standing wave ratio (VSWR) of 1.02 . For tuning purposes two screws were set in the coupler wall along the y-axis (x=0; y=±2b; z=0).

(a)

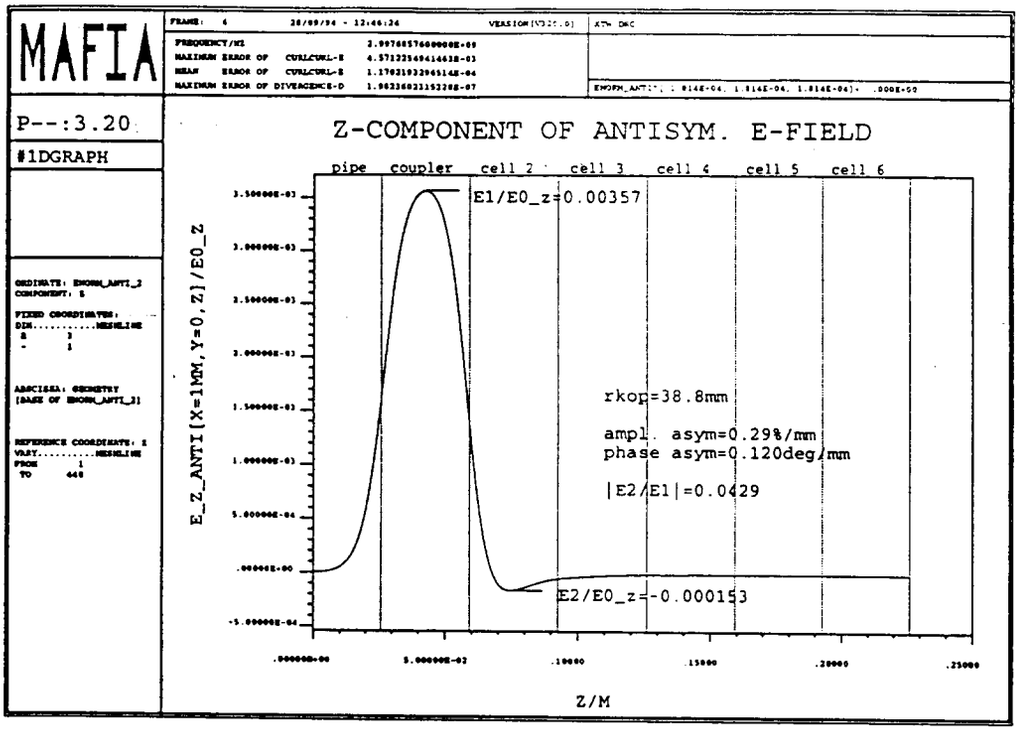

(b)

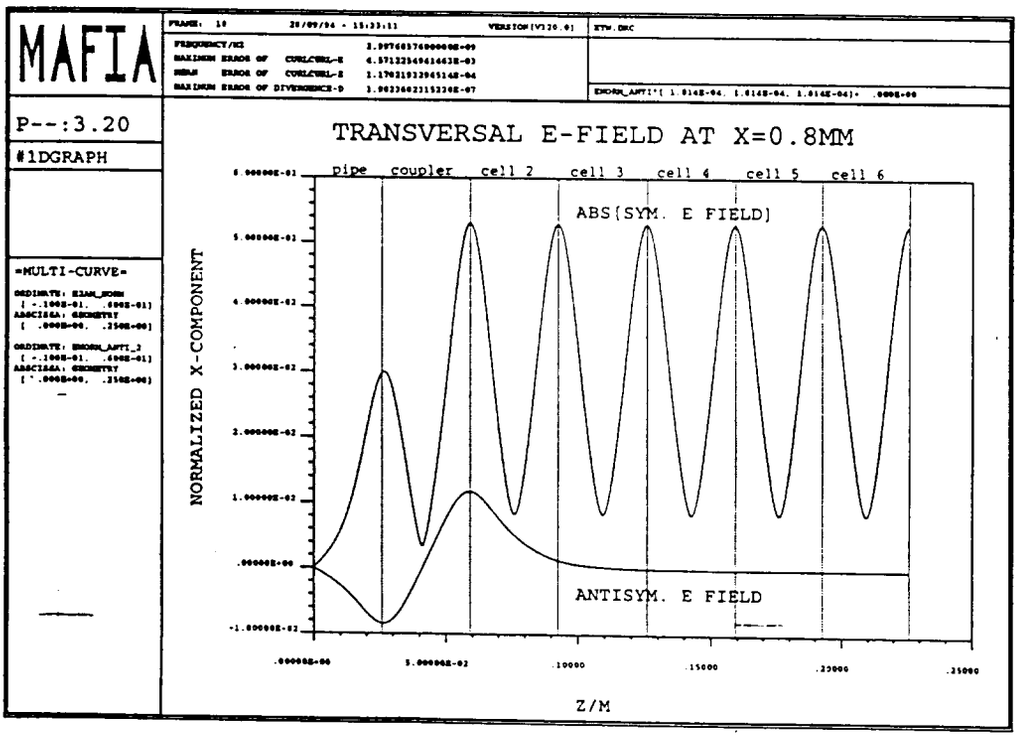

Fig. 8. The normalized antisymmetric and symmetric components of the E-field along the z-axis of the structure calculated by MAFIA:
(a) - Antisymmetric component of the longitudinal E-field;
(b) - Antisymmetric and symmetric componets of the transversal E-field at x=0.8 mm.

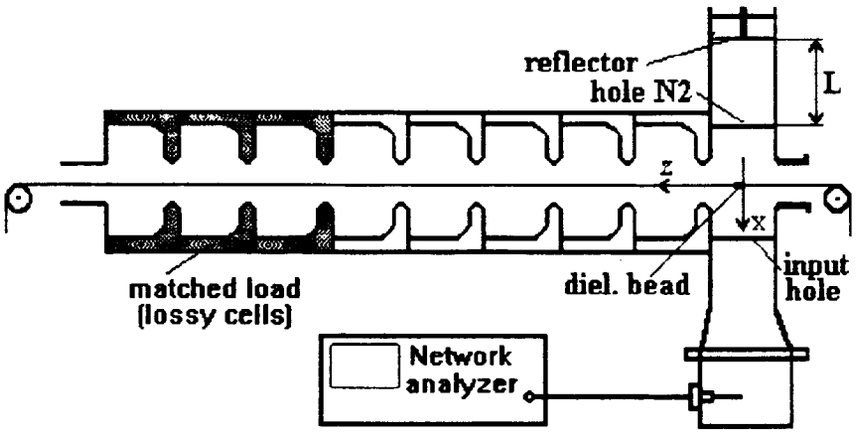

Fig. 9. The scheme of measurements on the traveling wave with matched load at the structure end.

The measurements of the field distribution in the coupler were carried out as before with 3 mm shift of the perturbation body along the x-axis for the different positions of the reflector. At first the measurements were made with the reflector in the initial position (L=75 mm), with that the matching condition of the coupler was realized. Then the measurements were repeated for different values of L (76,5 mm. 79 mm, 81 mm, 88,5 mm). To obtain the matching condition again, the coupler cell was tuned by metallic screws. The fine tuning is achieved by slight variation of L. This procedure is possible because the dimension of the input coupling hole to achieve matching is almost independent of the tuning of the coupler cell. For increasing values of L the screws must be turned into the coupler cavity in order to increase the frequency of this cell. The measured values of the normalized amplitude and phase are listed in tables 4, 5 and shown in figures 10, 11.

Table 4. The normalized field amplitude along the x-axis in the coupler (z=0 mm).

x , mm	normalized amplitude [E(x)/Eo] , Units				
	L=75 mm	L=76,5 mm	L=79 mm	L=81 mm	L=88,5 mm
-12	0,98635	0,99109	0,99519	1,00220	1,01029
-9	0,99066	0,99221	0,99587	1,00035	1,00837
-6	0,99179	0,99437	0,99598	0,99880	1,00404
-3	0,99505	0,99663	0,99655	0,99945	1,00033
0	1,00000	1,00000	1,00000	1,00000	1,00000
3	1,00671	1,00440	1,00478	1,00467	1,00165
6	1,01395	1,01506	1,00628	1,01037	1,00526
9	1,02236	1,01888	1,01460	1,01667	1,01012
12	1,03090	1,02622	1,02176	1,02211	1,01365

Table 5. The phase of the field along the x-axis in the coupler (z=0 mm).

x , mm	Phase [φ(x)-φ$_o$] . degrees				
	L=75 mm	L=76,5 mm	L=79 mm	L=81 mm	L=88,5 mm
-12	-0,254	0,161	-0,170	0,243	-0,374
-9	-0.602	-0,395	-0,312	-0,297	-0,622
-6	-0,584	-0,370	-0,712	-0,443	-0,694
-3	-0,448	-0,224	-0,387	-0,234	-0,584
0	0,000	0,000	0,000	0,000	0,000
3	0,578	0,571	0,664	0,846	0,377
6	1,220	1,563	1,014	1,758	1,528
9	2,359	2,337	2,255	2,839	2,614
12	3,567	3,588	3,552	4,087	3,422

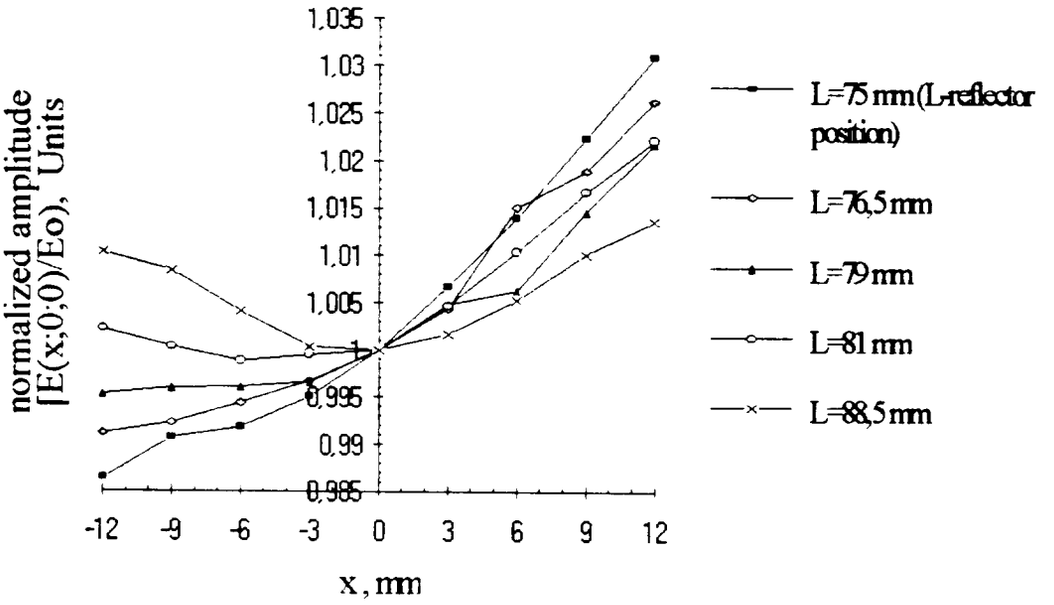

Fig. 14. The field amplitude along the x-axis in the coupler (z=0).

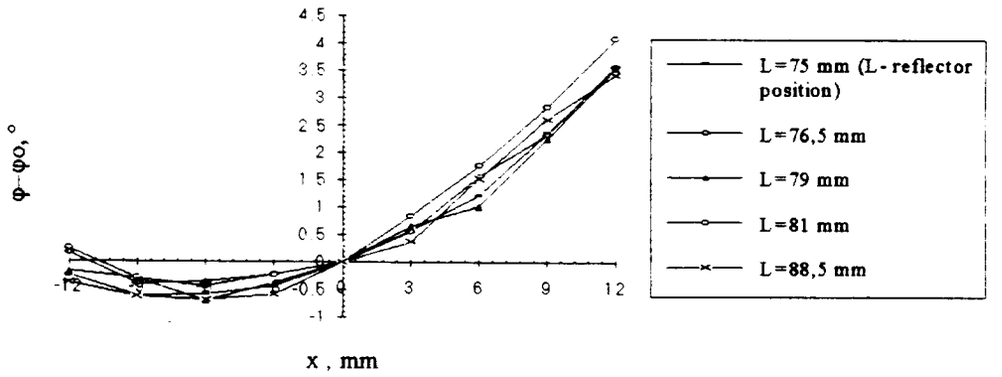

Fig. 15. The field phase [φ(x)-φ$_o$] along the x-axis in the coupler (z=0) .

The asymmetry of the field amplitude and phase in the coupler have been calculated by formulas (1) and (2) for different values of L. The calculated results are listed in tables 6 and 7. From these tables we can see that the field amplitude asymmetry is reduced with the increase of L and the decrease of the diameter ($2b$) of the coupler cell. With that the phase asymmetry is changed little.

Table 6. The field asymmetry in the coupler (z=0)

dx , mm	Field amplitude asymmetry , %/mm				
	L=75 mm	L=76,5 mm	L=79 mm	L=81 mm	L=88,5 mm
6	0.1942	0.1294	0.1371	0.0870	0.0219
12	0.1847	0.1724	0.0858	0.0965	0.0102
18	0.1761	0.1481	0.1041	0.0907	0.0097

Table 7. The phase asymmetry in the coupler (z=0)

dx , mm	Field phase asymmetry , °/mm				
	L=75 mm	L=76,5 mm	L=79 mm	L=81 mm	L=88,5 mm
6	0.171	0.132	0.175	0.180	0.160
12	0.150	0.161	0.144	0.183	0.185
18	0.165	0.152	0.143	0.174	0.180

This means that the amplitude asymmetry can be compensated completely for one set of geometrical parameters b, L , $h_1 = h_2$. This optimum can also be obtained for other dimensions of the second coupling hole (h_2) by choosing the appropriate reflector position L. As the length L can be determined experimentally, the correct values of b and h_1 are the basis for the optimization. For the next design step, we changed these parameters to b=38.2 mm and $h_1 = h_2$ =30.7 mm based on the numerical calculations described in the next section. (The dimension $h_1 = h_2$ of the coupling hole includes a safety margin and a tolerance of -0.3 mm .)

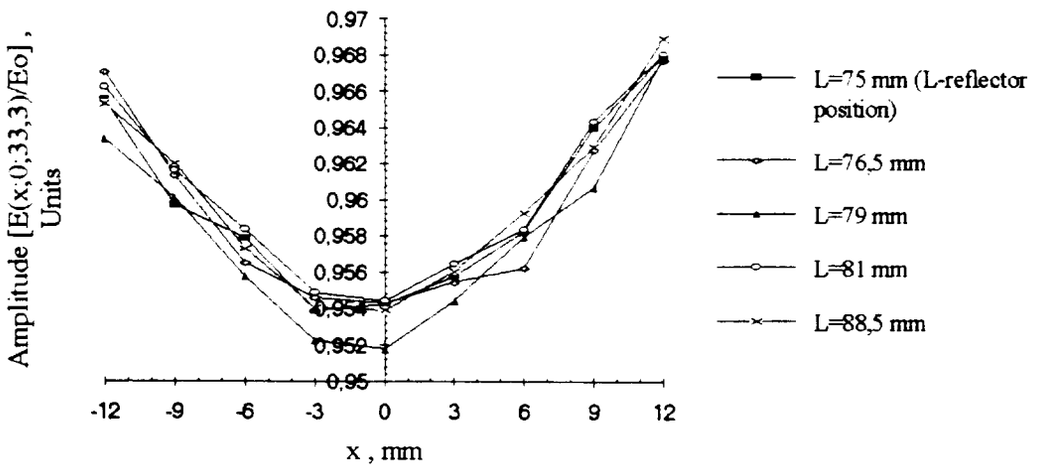

Fig.12. The field amplitude along the x-axis in the next cell after the coupler (z=33,3mm).

Figure 12 shows the field amplitude along the x-axis in the next cell after the coupler. As the asymmetry is theoretically very small, this data can be used to estimate the measurement accuracy: all values in table 8 are smaller than 0.035 % per mm. This is comparable to the accuracy estimation in section 2 of 0.05 % per mm.

Table 8. The field asymmetry in the next cell after the coupler (z=33,3 mm).

dx	Asymmetry , %/mm				
mm	L=75 mm	L=76,5 mm	L=79 mm	L=81 mm	L=88,5 mm
6	0.0310	0.0139	0.036	0.0268	0.0333
12	0.0029	0.0024	0.0185	0.0002	0.0165
18	0.0238	0.0079	0.0034	0.0150	0.0052

In fig.13 the variations of the amplitude asymmetry normalized to the field amplitude $E_0(x=0; y=0; z=0)$ are plotted along the z-axis of the structure for different reflector positions (L) of the matching coupler. With the exception of the coupler cell all values are dominated by measurement errors. Especially in the iris planes the measurement is very sensitive to transversal position errors due to the high field gradients calculated above and shown in fig.8b. With value L=88.5 mm for the reflector position the amplitude asymmetry in the coupler is almost the same as in the next cells and in 3÷5 times higher for the L=75 mm and 79 mm.

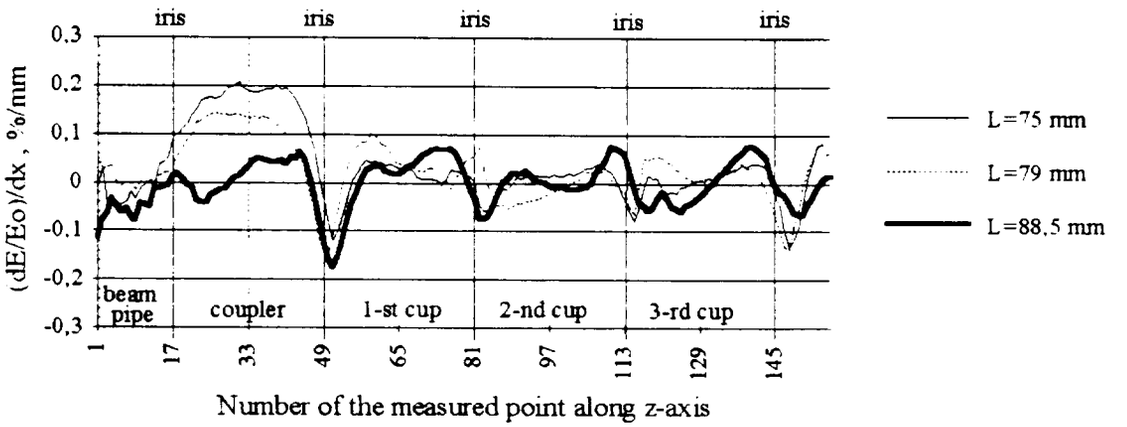

Fig. 13. The variation of the normalized amplitude asymmetry along the z-axis for different positions of the reflector. *L* - reflector position; a measurement step is 1, 01185 mm .

4. Calculation of the influence of the coupler geometry parameters on the asymmetry.

4.1. Two dimensional calculations.

The 3 dimensional geometry of the coupler together with the periodic structure can be separated into two parts that are only 2 dimensional.

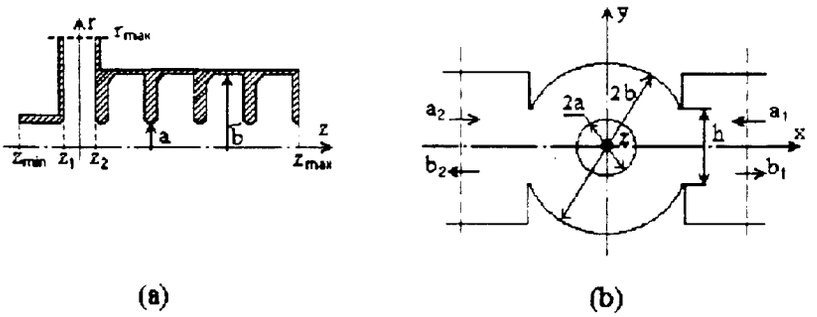

Fig. 14 (a). The coupler cell with the infinite radius and periodic structure in rz-coordinates.
(b). The coupler cell and the waveguides in the xy-coordinates.

The geometry in fig. 14(a) is independent of the coupler dimensions h, b, L and therefore has to be calculated only once. The traveling wave field $\vec{E}^{(a)}$ can be obtained as a linear combination of two standing wave fields $\vec{E}_{1/2}$ that fulfill the boundary conditions

$$\begin{aligned} & \vec{E}_1 \cdot \vec{e}_z = 0 \\ \text{or} \quad & \vec{E}_2 \times \vec{e}_z = \vec{0} \qquad \text{at} \quad z = z_{\max} \\ \text{and} \quad & \vec{E}_{1/2} \cdot \vec{e}_z = E_0 \qquad \text{at} \quad r = r_{\max},\ z_1 \le z \le z_2 . \end{aligned}$$

The traveling wave field is normalized to a power flow of 1W in the periodic structure. In the flat part of the structure (fig. 14(a), $z_1 \le z \le z_2$) the field can be described by the following expansion.

$$E_z^{(a)}(r,z) = \sum_{\nu} \left(A_\nu J_0(k_\nu r) + B_\nu H_0^{(2)}(k_\nu r) \right) \cos\left(\nu\pi \frac{z}{z_2 - z_1} \right) \qquad (4)$$

$$\textit{for } r>a \textit{ with } z\in[z_1,z_2];\quad k_\nu = \sqrt{\left(\frac{\omega}{c}\right)^2 - \left(\frac{\nu\pi}{z_2 - z_1}\right)^2}$$

Only the $\nu=0$ - term is not evanescent. For the calculation of the coupling only this term and therefore the coefficients A_0, B_0 have to be regarded.

The field in the coupler cell and the scattering parameters of the xy-configuration in fig. 14(b) can be characterized by the following equations:

$$E_z^{(b)}(r,\varphi) = (a_1 + a_2)\sum_{\substack{n=0 \\ \nu=2n}}^{\infty}\left(C_\nu J_\nu\left(\frac{\omega}{c}r\right) + D_\nu H_0^{(2)}\left(\frac{\omega}{c}r\right)\right)\cos\nu\varphi +$$

$$+(a_1 - a_2)\sum_{\substack{n=0 \\ \nu=2n+1}}^{\infty}\left(C_\nu J_\nu\left(\frac{\omega}{c}r\right)\right)\cos\nu\varphi +$$

$$+ \quad I \quad \sum_{\substack{n=0 \\ \nu=2n}}^{\infty}\left(E_\nu J_\nu\left(\frac{\omega}{c}r\right) + F_\nu H_0^{(2)}\left(\frac{\omega}{c}r\right)\right)\cos\nu\varphi \quad , \tag{5}$$

$$\begin{pmatrix} b_1 \\ b_2 \end{pmatrix} = \begin{pmatrix} \tilde{s}_{11}\,\tilde{s}_{12} \\ \tilde{s}_{12}\,\tilde{s}_{11} \end{pmatrix}\begin{pmatrix} a_1 \\ a_2 \end{pmatrix} + \begin{pmatrix} \alpha \\ \alpha \end{pmatrix}\cdot I \tag{6}$$

All coefficients C_ν, D_ν, E_ν, F_ν, $\tilde{s}_{11}$, $\tilde{s}_{12}$, α can be evaluated by multimode expansion from only 3 field calculations with

1). $a_1 + a_2 = 1$, $a_1 - a_2 = 0$, $I=0$;
2). $a_1 + a_2 = 0$, $a_1 - a_2 = 1$, $I=0$;
3). $a_1 + a_2 = 0$, $a_1 - a_2 = 0$, $I=1$,

but in this context we need only C_0, D_0, E_0, F_0, $\tilde{s}_{11}$, $\tilde{s}_{12}$, α to calculate the scattering parameters S_{11}, S_{12} of the 3 dimensional coupler with infinite traveling wave structure.

First we analyze the symmetric operation with $a_1 = a_2$: as the higher order terms decay in (4) for $r>>a$ and in (5) for $r<<b$ the coupling is essentially caused by the lowest order terms $\nu=0$. The comparison of these coefficients leads to

$$\begin{pmatrix} A_0 \\ B_0 \end{pmatrix} = \begin{pmatrix} C_0\,E_0 \\ D_0\,F_0 \end{pmatrix}\begin{pmatrix} 2a_1 \\ I \end{pmatrix} \tag{7}$$

In the antisymmetric modus $a_1 = -a_2$ the coupler cell is nonresonant and no traveling wave can propagate into the periodic structure. Due to this fact the reflection of the 2 dimensional structure in fig. 14(b) is a very good approximation for the 3 dimensional behavior:

$$b_{1/2} = \pm(\tilde{s}_{11} - \tilde{s}_{12})\, a_{1/2} \tag{8}$$

Combining the equations (6) to (8) we can derive the scattering equation of the 3 dimensional coupler:

$$\begin{pmatrix} b_1 \\ b_2 \end{pmatrix} = \underbrace{\left\{ \begin{pmatrix} \tilde{s}_{11} & \tilde{s}_{12} \\ \tilde{s}_{12} & \tilde{s}_{11} \end{pmatrix} + \alpha \frac{F_0 A_0 - E_0 B_0}{-D_0 A_0 + C_0 B_0} \begin{pmatrix} 1 & 1 \\ 1 & 1 \end{pmatrix} \right\}}_{\begin{pmatrix} S_{11} & S_{12} \\ S_{12} & S_{11} \end{pmatrix}} \begin{pmatrix} a_1 \\ b_1 \end{pmatrix}$$

By this method we analyzed the configuration for several sets of parameters (b, h) and tested whether reflector positions L exist, that fulfill the matching condition:

$$r_1 := \frac{b_1}{a_1} = 0$$

Therefore the coupler must be terminated at the second port by

$$R := \frac{a_2}{b_1} = \frac{S_{11}}{\det S}.$$

The curve of possible (b, h) pairs with $R=-exp(-2\beta L)$ is plotted in fig. 15.

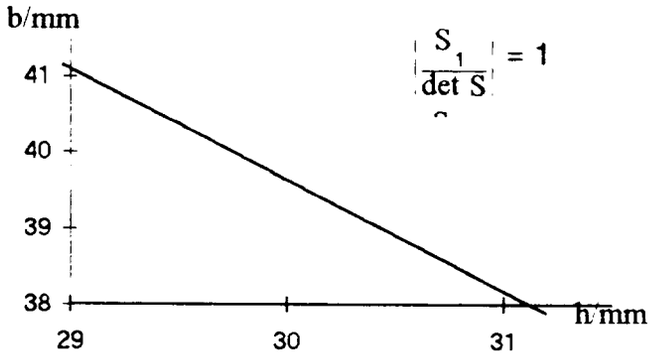

Fig.15. Possible (b, h) values, for which the coupler can be matched by tuning L.

With these 2D results it is possible to calculate the asymmetry up to a multiplicative factor. This factor depends approximately linearly on h and due to the small variations in this parameter we will treat it as a constant. Its value can be calculated by a single 3D calculation.

The field in the coupler and the connected periodic structure can be expressed as a linear combination of a pure symmetric field $\vec{E}^+$ with $a_1=a_2=a^+$ and a pure antisymmetric field $\vec{E}^-$ with $a_1=-a_2=a^-$.

$$\vec{E} = \frac{a_1 + a_2}{2} \frac{\vec{E}^+}{a^+} + \frac{a_1 - a_2}{2} \frac{\vec{E}^-}{a^-} = a_1 \left\{ \left(1 - \frac{1}{2} \cdot \frac{1}{1 - R(S_{11} - S_{22})} \right) \cdot \frac{\vec{E}^+}{a^+} + \frac{1}{2} \cdot \frac{1}{1 - R(S_{11} - S_{22})} \cdot \frac{\vec{E}^-}{a^-} \right\}$$

As S_{11}, S_{12} and $R=S_{11}/\det S$ are know, only $\frac{\vec{E}^+}{a^+}$ and $\frac{\vec{E}^-}{a^-}$ have to be evaluated to obtain the complete field information. For the asymmetry

$$A = \left.\frac{dE_z/dz}{E_z}\right|_{x=y=0} = \frac{\frac{1}{2}\cdot\frac{1}{1-R(S_{11}-S_{22})}\cdot\frac{dE_z^-/dz}{a^-}}{\left(1-\frac{1}{2}\cdot\frac{1}{1-R(S_{11}-S_{22})}\right)\cdot\frac{E_z^+}{a^+}}$$

we need only the "on axis " values of $\frac{E_z^+}{a^+}$ and $\frac{dE_z^-/dz}{a^-}$. The longitudinal field

$$E_z(x=y=0,z) = a_1\left(1-\frac{1}{2}\cdot\frac{1}{1-R(S_{11}-S_{22})}\right)\cdot\frac{E_z^+}{a^+}$$

is identical to the monopole field of the configuration in fig. 14(a) $E_z^{(a)}(r=0, z)$. As a_1 is known by equation (7), we can evaluate E_z^+/a^+. The antisymmetric field $\vec{E}^-/a^-$ is a nonresonant standing wave field that is evanescent in the periodic structure. A rough estimation of the amplitude and a good estimation of the phase can be obtained by analyzing the field of the configuration in fig.14(b) with $a_1=a_2=a^-$, $I=0$.

A better estimation is possible by calculating the 3D structure with only a few cells of the periodic structure. As $\frac{dE_z^-/dz}{a^-}$ varies much less for the geometrical changes in this investigation (30.2 mm < h < 31.2 mm, $b(h)$, see fig.15), this value has been calculated only once.

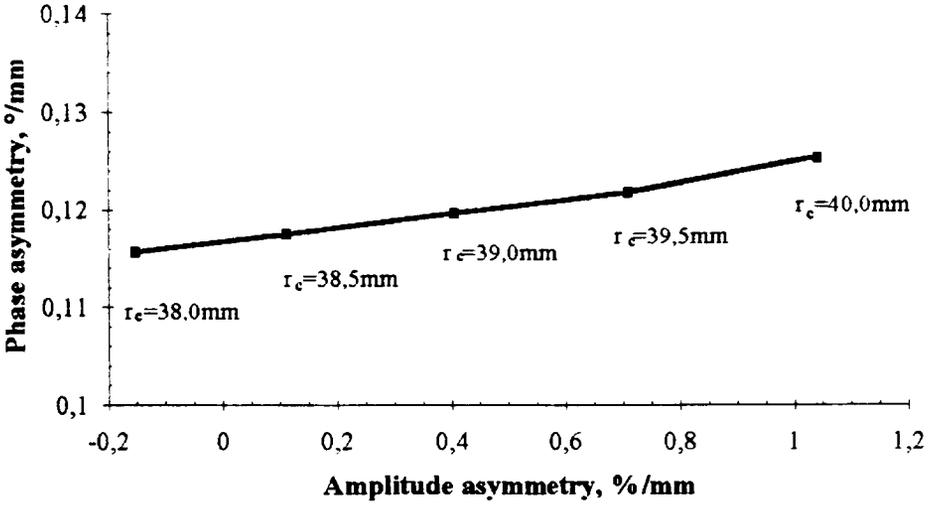

Fig. 16 Variation of the amplitude and phase asymmetry dependent on the cavity radius ($r_c \equiv b$) and for optimal values of h and L.

In fig. 16 the amplitude and phase asymmetry for b= 38.0÷40.0 mm are plotted. The phase asymmetry is weakly dependent on the geometrical variation while the asymmetry of the amplitude can be compensated for b=38.25mm.

4.3. Three dimensional calculation.

As no software tool is available for a direct calculation of the field in a coupler connected to an infinite traveling wave structure, either calculations very similar to those for the configuration in fig.14(a) have to be carried out or an input coupler, a few cells and an output coupler have to be modeled. In both cases the numerical effort is approximately two orders higher than for the 2D-calculations. Therefore only one geometry with b=38.2 mm has been analyzed by the second method: input coupler - cell - output coupler. Figures 17 and 18 show the amplitude and phase along the x-axis for y=z=0. The amplitude asymmetry -0.06 % per mm and the phase asymmetry +0.131 ° per mm are comparable to the results of the 2D-calculation (-0.05 % per mm, 0.12 ° per mm). The electrical field strength in the waveguide at the second port does not exceed the values of the waveguide from the RF-source. The left field maximum (closer to the reflector) is slightly higher than the right one. This means, that the amplitude asymmetry is over compensated. The clear phase change in the right side of the input cavity indicates a traveling wave while the left side is almost in a standing wave regime as there is no power flow from the second waveguide.

5. The transverse momentum.

The transverse momentum has been estimated in [5]. Using the same approximations and the formulas (1) and (2) we can write

$$\delta p_x(\Delta\varphi) = p_0 \frac{c}{\omega}\left[\frac{\pi}{180°} A_\varphi \cos\Delta\varphi + \frac{A_a}{100\%}\sin\Delta\varphi\right].$$

Here $p_0 = eE_0\, d/c$ is the longitudinal moment caused by the accelerating field in one cell and $\Delta\varphi$ is the phase shift relative to the crest of the wave. For bunches short compared to the wavelength the phase asymmetry causes a constant transverse momentum which can (for example) be compensated by a correction coil. In Linac II the bunch length is typically ±20° and a fraction of the particles is accelerated off crest. Therefore a transverse momentum due to an amplitude asymmetry can occur, depending on the position (or say: a phase) of the particle relative to the crest. Nevertheless the amplitude asymmetry in the Linac II coupler can be compensated down to 0.05 %/mm and has a negligible effect.

(a)

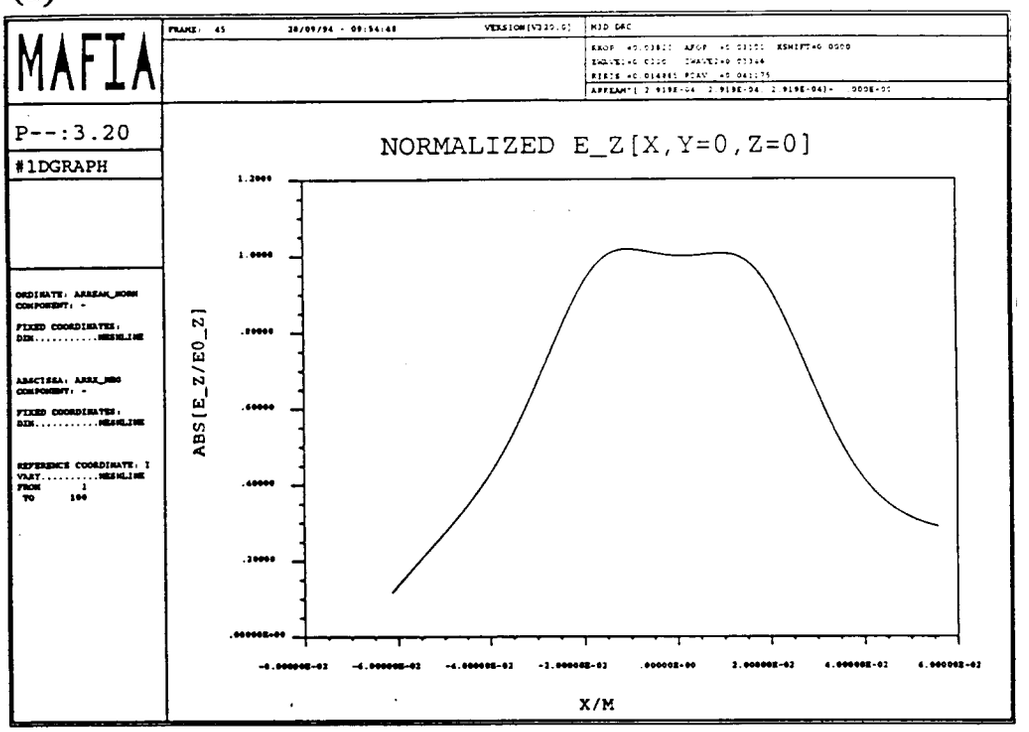

(b)

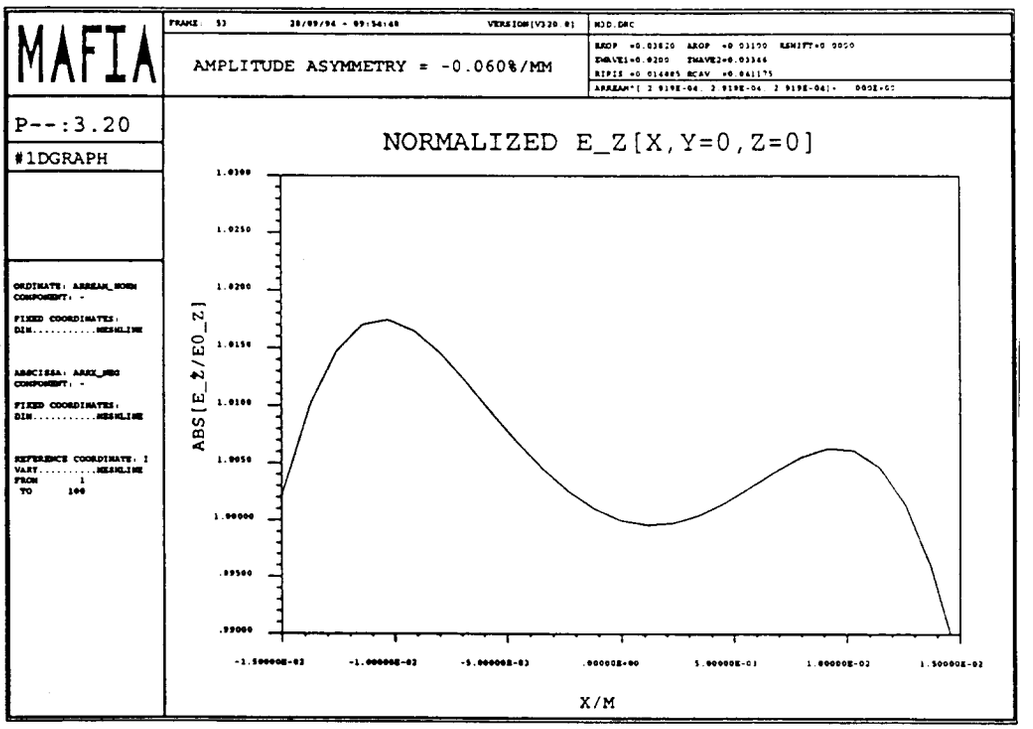

Fig.17. Amplitude of the z-component of the electrical field in an input coupler along the x-axis:

(a) - Range of the x-axis from the reflector through the coupler cell into the input waveguide;

(b) - Magnified range of the x-axis along the iris hole.

(a)

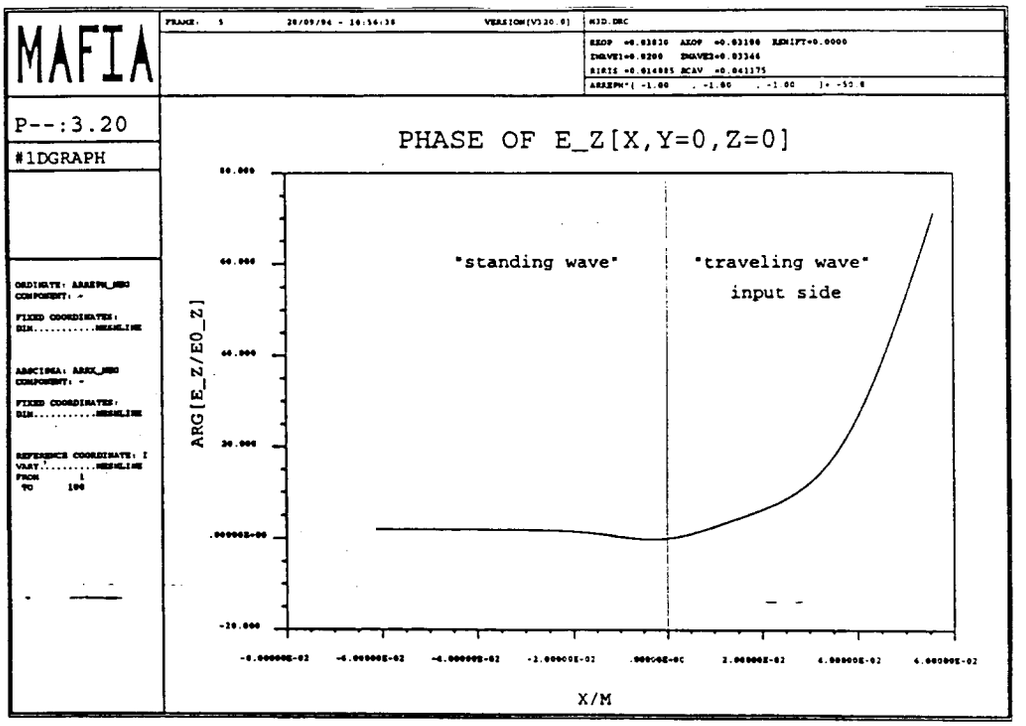

(b)

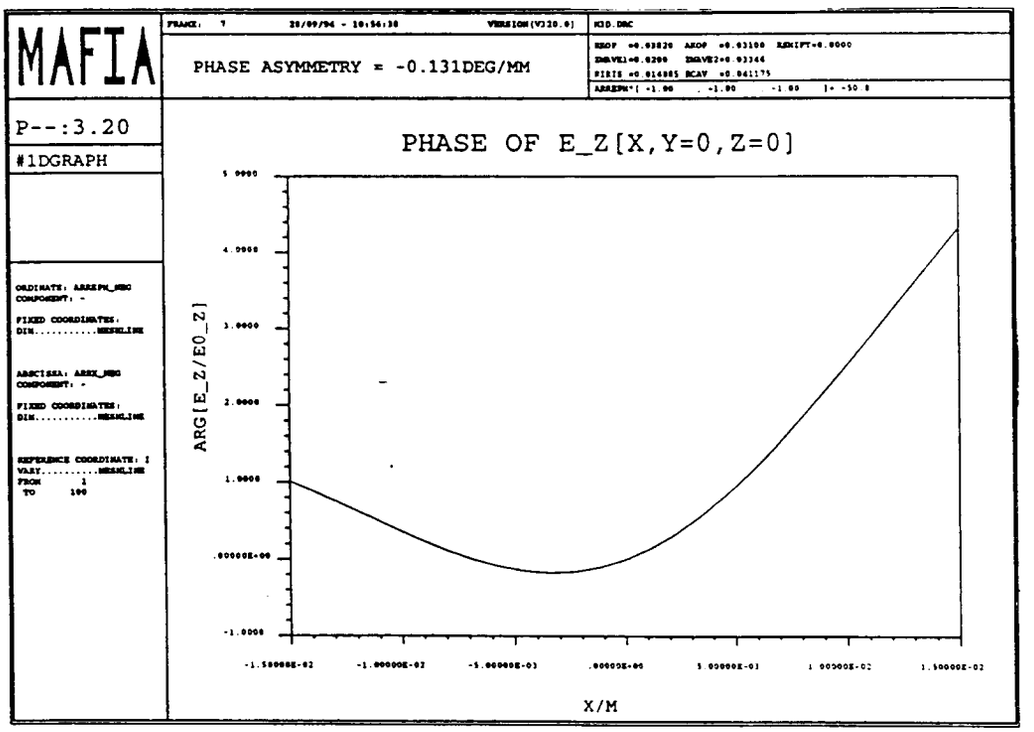

Fig.18. Phase of the z-component of the electrical field in an input coupler along the x-axis:

(a) - Range of the x-axis from the reflector through the coupler cell into the input waveguide;

(b) - Magnified range of the x-axis along the iris hole.

6. Conclusion

The asymmetry of the symmetric two-hole-coupler, which is terminated on one port by an adjustable reflector, has been calculated and investigated. The field asymmetry in the coupler cell is 0.2÷0.3 % per mm and the phase asymmetry is 0.1÷0.2 °/mm for the optimum position of the plunger. The asymmetry decreases about one order of magnitude per cell. By increasing the resonance frequency of the coupler cell (by reducing the diameter $2b$ or the N2 hole aperture seen in fig. 1) and matching the system by changing the reflector position (L) the amplitude asymmetry can be compensated completely, while the phase asymmetry remains almost unchanged. Based on these investigations the geometry of the coupler has been changed for the next design step. An amplitude asymmetry below 0.05 %/mm and a phase asymmetry of $0.13 \div 0.15$ ° per mm are expected.

6. Reference

[1]. Varian Associates, Palo Alto, CA, USA, 1970.

[2]. J. Haimson, *Collinear Termination for High Energy Particle Accelerators*, June, 1961, US-Patent Nr. 3264515.

[3]. Ch. W. Steele, *A Nonresonant Perturbation Theory*, IEEE Trans. on Microwave Theory and Techniques, Vol. MTT14, Nr.2, Feb. 1966.

[4]. G. Kreps, DESY, private communication

[5]. G.A.Loew and R.B.Neal, *Accelerating Structures*, Chapter B.1.1; "Linear Accelerators", P.M.Lapostolle and A.L.Septier, Eds. North Holland Publishing Company., 1970.